Localized state in a two-dimensional quantum walk on a disordered lattice

Peng Xue,[1,*] Rong Zhang,[1] Zhihao Bian,[1] Xiang Zhan,[1] Hao Qin,[1] and Barry C. Sanders[2,3,4,5]
[1]*Department of Physics, Southeast University, Nanjing 211189, China*
[2]*Hefei National Laboratory for Physical Sciences at Microscale and Department of Modern Physics, University of Science and Technology of China, Hefei, Anhui 230026, China*
[3]*Shanghai Branch, CAS Center for Excellence and Synergetic Innovation Center in Quantum Information and Quantum Physics, University of Science and Technology of China, Shanghai 201315, China*
[4]*Institute for Quantum Science and Technology, University of Calgary, Alberta, Canada T2N 1N4*
[5]*Program in Quantum Information Science, Canadian Institute for Advanced Research, Toronto, Ontario, Canada M5G 1Z8*
(Received 9 May 2015; published 14 October 2015)

We realize a pair of simultaneous ten-step one-dimensional quantum walks with two walkers sharing coins, which we prove is analogous to the ten-step two-dimensional quantum walk with a single walker holding a four-dimensional coin. Our experiment demonstrates a ten-step quantum walk over an 11×11 two-dimensional lattice with a line defect, thereby realizing a localized walker state.

DOI: 10.1103/PhysRevA.92.042316 PACS number(s): 03.67.Ac, 05.40.Fb, 42.50.Xa, 71.55.Jv

I. INTRODUCTION

Quantum walks (QWs) [1], which are the quantum analog of classical random walks (RWs), are valuable in diverse areas including quantum algorithms [2–5], quantum computing [6–8], state transfer and quantum routing [9], quantum simulation [10], topological phase transition [11–13], energy transport in photosynthesis [14,15], Anderson localization [16–25], and quantum chaos [26–30]. The one-dimensional (1D) QW has been realized with nuclear magnetic resonance [31], atoms [32–37], and photons [38–42]. Notably the 1D QW has a classical-wave description [43–45], whereas the two-dimensional (2D) QW [46–48] introduces purely quantum effects [49]. Consequently, the 2D QW over integer time t is of paramount interest motivating recent photonic realizations [10,22,50–52] that are actually constructed with a pair of 1D QWs and presume a relation between two 1D QWs and one 2D QW.

Here we demonstrate experimentally a QW localized state by realizing a line defect in the reduced QW position distribution $\tilde{P}_t^{xy}$ over an 11×11 2D (x,y) lattice and compare to the theoretical prediction P_t^{xy}. We use a tilde to denote experimental quantities, superscripts x and y to denote lattice sites x and y, and subscript t to denote the time index. The localized state of the walker as a signature of 2D QW localization presents the property as the probability distribution of the walker state is highly localized in certain positions instead of spreading. In additional we prove an isomorphism between a pair of 1D QWs sharing coins [49] and a single 2D QW on an integer-valued Cartesian (x,y) lattice (see Appendix). Our proof of the isomorphism between two walkers in one dimension sharing coins and one walker in two dimensions with a higher-dimensional coin makes rigorous an oft-used but previously unproven assumption of this isomorphism.

We evaluate the quality of experimental simulation in terms of the time-dependent discrepancy

$$s_t = \frac{1}{2}\sum_{x,y}\left|\tilde{P}_t^{xy} - P_t^{xy}\right|, \tag{1}$$

using the 1-norm distance [53] between theoretical and experimental reduced walker distribution on the 2D lattice. In particular, we show that the discrepancy s_t is small for our realization, indicating a successful experimental simulation of a localized state in a 2D QW.

II. THEORY: LOCALIZATION IN A QUANTUM WALK

Compared to ballistic QWs, a walk in a disordered lattice leads to an absence of diffusion, and the wave function of the walker becomes localized [54]. That is, the walker will be observed in a certain position with high probability instead of spreading ballistically. Thus the localized state of the walker is good evidence for observing a localized QW.

The unitary operation for a single step of QW in a disordered lattice shown in Fig. 1(a) is

$$V_t^{2\mathrm{D}}(\phi) = \sum_{x,y\in\Delta_t}\sum_{c,d\in\mathbb{B}} e^{i\phi(x,y)}|x+(-1)^c, y+(-1)^d\rangle\langle x,y| \otimes |c,d\rangle\langle c,d| H^{\otimes 2}, \tag{2}$$

where $H = \begin{pmatrix}1 & 1\\ 1 & -1\end{pmatrix}/\sqrt{2}$ is a Hadamard coin operator. In this paper we consider two types of disorders that are represented by position-dependent string phase defects $e^{i\phi(\delta_{x,0}+\delta_{y,0})}$ and $e^{i\phi\delta_{y,0}}$ with $\delta_{x(y),0}$ the Kronecker δ.

The first type of disorder corresponds to the case that the first (second) walker is controlled by a Hadamard coin, walks along x (y) direction, and obtains an additional phase ϕ whenever passing through $x=0$ ($y=0$). In contrast, the second case corresponds to the case that the second walker obtains an additional phase whenever passing through $y=0$. Both cases break the translational symmetry of the standard QW without creating defects.

Compared to the standard QW, which can be factorized into two independent distributions of 1D Hadamard QWs as shown in Fig. 1(b), the 2D QW with position-dependent string phase defect shows a completely different position distribution as shown in Figs. 1(c) and 1(d). A QW with phase defects on $y=0$ is topologically equivalent to that with a walker on a 2D regular lattice that is trapped on line $x=0$. On the other hand, a QW with phase defects on $x(y)=0$, the QW is topologically

*gnep.eux@gmail.com

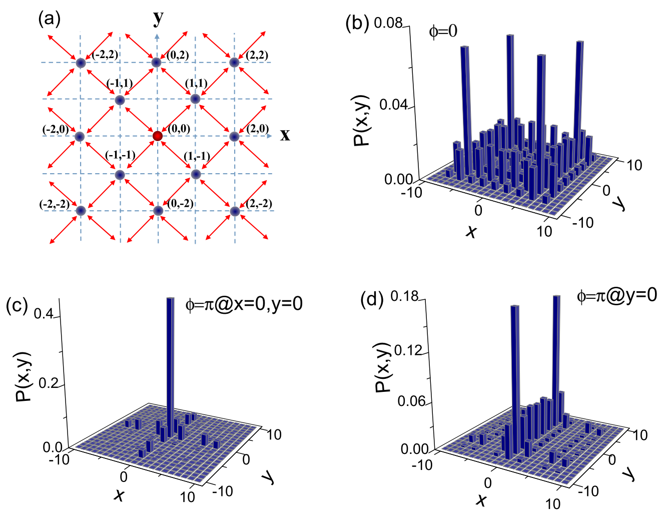

FIG. 1. (Color online) (a) The 2D lattice of vertices that represent the state space of two walkers populating an 11×11 position lattice in an interferometer network. (b) Theoretical position distribution after ten steps of a homogeneous 2D Hadamard QW. (c) Theoretical position distribution after ten steps of a 2D Hadamard QW with line phase defects $\phi = \pi$ on both $x = 0$ and $y = 0$. (d) Theoretical position distribution after ten steps of a 2D Hadamard QW with line phase defects $\phi = \pi$ only on $y = 0$.

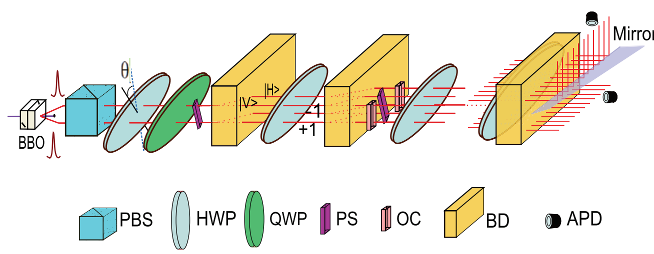

FIG. 2. (Color online) Detailed sketch of the setup for ten-step 2D QW with position-dependent phase defect ϕ on $x(y) = 0$. Photon pairs created via type-I SPDC are injected to the optical network from different ports. Arbitrary initial coin states are prepared via a PBS, HWP, and QWP. PSs are placed in the corresponding spatial modes and the optical compensators (OCs) are used to compensate the temporal delay caused by PSs. Coincident detection of photons at the APDs (7 ns time window) predicts a successful run of the QW.

equivalent to that with a walker is localized on lines $x(y) = 0$. The maximal probability of the walker appears at the junction point (0,0).

III. EXPERIMENT

Here we simulate experimentally a 2D photonic walk with 1D QW by realizing two walkers passing through a disordered lattice and employing the separable coin operation $H^{\otimes 2}$. We simulate two kinds of disordered lattices: (i) a single-point phase defect in the original position (0,0) and (ii) a string phase defect in the axis $y = 0$. In this way we can observe localization both (i) on a single point and (ii) on a line.

A. Positions of one-dimensional walkers

QWs can be produced by photons passing through a cascade of birefringent calcite beam displacers (BDs) arranged in a network of Mach-Zehnder interferometers [24,28,30]. The direction of the single-photon transmission is controlled by the coin state, i.e., physically the photon polarization.

Each interferometric output corresponds to a given point in the space and time location of the 1D QW. Here for 2D QW, pairs of photons are created via spontaneous parametric down conversion (SPDC) and then injected separately into the interferometer network from different input ports. They do not interfere with each other. Pairs of photons propagate along x and y axes, respectively, which correspond to the four different directions taken by single photon in one step on a 2D lattice.

In this scenario, disorder can be added in the evolution by simply introducing polarization-independent phase shifters (PSs) between the interferometer paths. Benefiting from the novel technology of PSs applied in arbitrary positions and the stability of the BD interferometer network, we are able to realize a ten-step 2D QW within an 11×11 lattice influenced by various types of controllable disorders. With this instrument, we observe that photon wave functions are trapped not only at single points but also on lines. Furthermore, these defects can be used to implement arbitrary phase maps in QWs.

B. One quantum-walk step

In our experiment the setup in Fig. 2 has been realized by using the BD array as an interferometer network similar to that used in [24,28,30]. By taking advantage of the intrinsically stable interferometers, our approach is robust and able to control both coins and walkers at each step. Benefiting from the fully controllable implementation, we experimentally study the impact of the position-dependent phase defects on the localization effect in a QW architecture and the experimental results agree with the theoretical predictions. Compared to the previous experimental results which only simulated localization effect by trapping the walker in a certain single point [22–24], we experimentally localize the walker on the lines instead.

The challenge of our experiment is to realize a specific polarization-independent phase at each site via microscope slides (PSs) with precise effective thickness and to keep high interference visibility even with phase defect. Specifically, we rotate the PSs for each step and then gather the photon-count data.

These data are compared to the theoretical predictions. If the data are not satisfactory with respect to the 1-norm distance s_t of the walker distribution, we discard the data, adjust the PSs, and repeat. This postselection-like method provides an excellent agreement between the measured probability distribution (measured position variance) and theoretical prediction. By introducing controllable PSs in the paths of the interferometers, we have managed to create these versatile interferometer networks which can be used in many other fields.

C. Source and detection

The photon pairs generated via type-I SPDC in 0.5-mm-thick nonlinear-β-barium-borate crystal cut at 29.41°, pumped by a 400.8 nm cw diode laser with up to 100 mW of power. For 2D QWs, photon pairs at wavelength 801.6 nm are prepared into a symmetric initial state $[(|H\rangle + i|V\rangle)/\sqrt{2}]^{\otimes 2}$ via a polarizing beam splitter (PBS) followed by wave plates. Interference filters determine the photon bandwidth 3 nm and then pairs of down-converted photons are steered into the different optical modes (up and down) of the linear-optical network formed by a series of BDs, half-wave plates, and PSs.

Output photons are detected via avalanche photodiodes (APDs) with dark count rate of $<100\ \mathrm{s}^{-1}$ whose coincident signals—monitored using a commercially available counting logic—are used to postselect two single-photon events. The total coincident counts are about $300\ \mathrm{s}^{-1}$ (the coincident counts are collected over 60 s). The probability of creating more than one photon pair is less than 10^{-4} and can be neglected.

The coin state is encoded in the polarization $|H\rangle$ and $|V\rangle$ of the input photon. In the basis $\{|H\rangle,|V\rangle\}$, the Hadamard operator is realized with a HWP set to $\pi/8$. The walkers' positions are represented by longitudinal spatial modes. The unitary operator shown in Eq. (1) manipulates the wave packet to propagate according to the polarization of the photons. The translational symmetry of an ideal standard QW without defects is now broken by modifying the phase of the walkers on each site, which can be realized by simply introducing PSs in the specific interferometer arms. By adjusting the relative angle between the PS and the following BD, the effective thickness of the PS changes and the specific phase ϕ can be realized.

The spatial modes are separated by a BD with length 28.165 mm and clear aperture 33 mm × 15 mm. The optical axis of each BD is cut so that vertically polarized light is directly transmitted and horizontal light undergoes a 3 mm lateral displacement into a neighboring mode which interferes with the vertical light in the same mode. Each pair of BDs forms an interferometer. Only odd (even) sites of the walker are labeled at each odd (even) step, as the probabilities of the walker appearing on the other sites are zero. Pairs of photons are injected from different ports and propagate in different layers of the BD interferometer network.

The first ten steps of the QW with position-dependent phase defect ϕ applied on the two axes $x = 0$ and $y = 0$ are shown in Fig. 2. For each walker (photon), the longitudinal spatial modes after the first step are recombined interferometrically at the second step. The interference visibility is reached 0.998 per step (extinction ratio 1000 : 1). In both layers of the BDs the photons emerge in the $N + 1$ spatial modes at the output of the Nth step and are subsequently detected by an APD. The probabilities $P(x,y)$ are obtained by normalizing photon counts via a coincidence measurement for two walkers at position x and y, respectively, to total number of photon counts for the respective step.

The measured probability distributions for one to ten steps of a 2D Hadamard QW with position-dependent phase defect $\phi = \pi$ on $x(y) = 0$ and the symmetric initial coin state are shown in Fig. 3(a). The 1-norm distance is 0.095 ± 0.016 ensuring a good agreement between the measured probabilities and theoretic predictions after ten steps. The walkers' state after ten steps clearly shows the characteristic shape of a localization distribution: the wave functions of photons are trapped on two axes $x = 0$ and $y = 0$, and a pronounced peak of the probability 0.424 ± 0.015 (with theoretical prediction 0.441) in the junction point (0,0). In contrast to the ideal standard 2D Hadamard QW the expansion of the wave packet is highly suppressed and the probabilities $P(x,0)$ and $P(0,y)$ are enhanced. The maximal probability occurs at the junction point (0,0), which displays the signature of the localization effect.

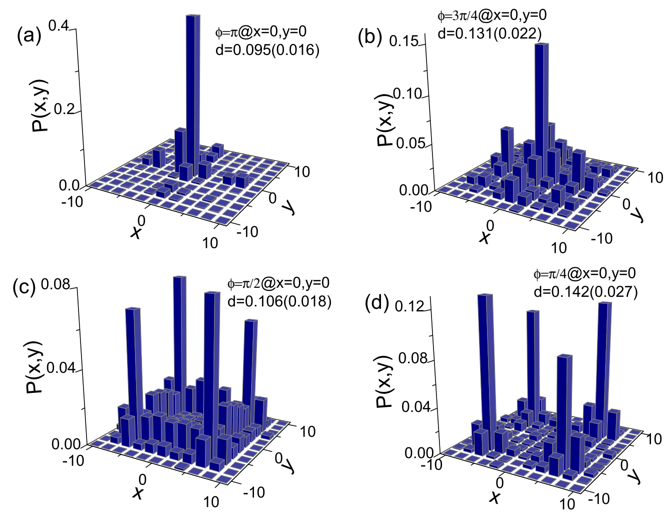

FIG. 3. (Color online) Experimental data of probability distributions of the ten-step 2D Hadamard QW with position-dependent string phase defects on both $x = 0$ and $y = 0$: (a) $\phi = \pi$, (b) $\phi = 3\pi/4$, (c) $\phi = \pi/2$, and (d) $\phi = \pi/4$. The walkers start from the original position (0,0) with the symmetric coin state.

D. Results

Our experimental result highlights the full control of the implementation of the 2D QW. In Fig. 3, we show the impact of phase defects $\phi \in [0,\pi]$ on the localization effect. Figures 3(b) and 3(d) show the position distribution of the ten-step 2D Hadamard QW with $\phi = 3\pi/4,\pi/2,\pi/4$. For the symmetric initial coin state, the two walkers behave the same and show the symmetric distributions.

The localization effect can be observed in the range $\phi \in [3\pi/4,\pi]$, and the recurrence probability $P_{10}(0,0)$ increases with ϕ, which agrees with the analytic result. Especially for $\phi = \pi$ the walkers are almost completely trapped on the axes x and y. If ϕ decreases, the 2D QW's behavior tends to be ballistic. For $\phi = \pi/2$ the wave functions of photons are distributed the same as for the standard Hadamard QW without phase defects. For $\phi = \pi/4$, the photons spread even faster and show a superballistic behavior.

Thus, whether or not the localization effect can be observed depends on the choices of phase defects. The dependence of the localization effect on ϕ can be explained [16,17] by the overlap between the localized eigenstates of the unitary step operation U and the initial state of the system.

Now we add the phase defects only on the y axis. That is, if and only if the walker who walks along the y axis arrives at $y = 0$ obtains an additional phase ϕ. Experimentally we

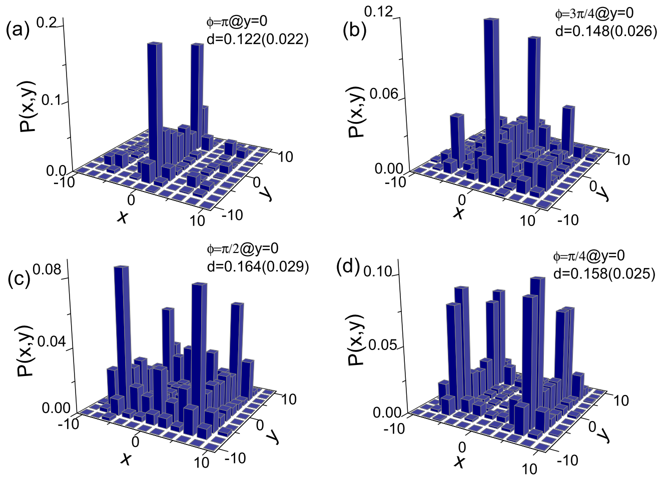

FIG. 4. (Color online) Experimental data of probability distributions of the ten-step 2D Hadamard QW with position-dependent string phase defects only on $y = 0$: (a) $\phi = \pi$, (b) $\phi = 3\pi/4$, (c) $\phi = \pi/2$, and (d) $\phi = \pi/4$.

rearrange the PSs and photons propagating in the lower layer pass through the PSs. In Fig. 4 we show the measured position distribution of 2D QW with the string phase defects, which displays that the photons appear on a line with relative large probabilities.

Thus, the photons are localized on the x axis for ϕ large enough. On the x axis, the photon distribution is similar to that of the 1D standard Hadamard QW. In Fig. 5, measured position variances of the walker along the y axis show the impact of phase defects. For $\phi = \pi/2$ photons show a ballistic behavior. For $\phi = \pi/4$ they move even faster and show a superballistic behavior. For $\phi = 3\pi/4$ and $\phi = \pi$ they stagnate and show localization. For $\phi = \pi$ the variances are even smaller than those of the classical RW, whereas the walker walking along the x axis is not influenced.

The performance of our setup is limited only by imperfections of the optical components such as nonplanar optical surfaces and the coherence length of single photons, resulting in errors and decoherence. A limitation for the maximal step number is given by the size of the clear aperture of the BDs. However, this problem is not intrinsic to this implementation,

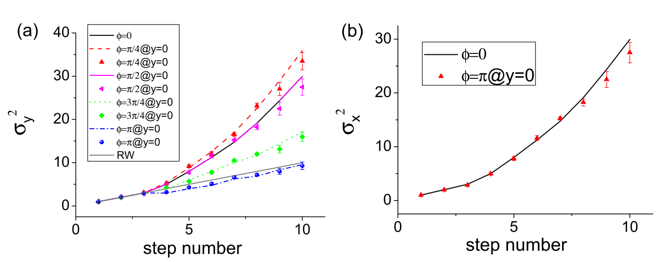

FIG. 5. (Color online) (a) Measured trend of the variance of the walker who walks along the y axis up to ten steps with respective theoretical predictions (lines). (b) Measured dynamics evolution of the position variance of the walker who walks along the x axis. As the phase defects are only applied on $y = 0$, the walker along the x axis is not affected. Thus for all ϕ the walker shows a ballistic behavior.

as the BDs with large enough clear aperture and strictly planar surface can realize the large-step QW.

IV. CONCLUSIONS

Our experimental architecture can be generalized to more than two dimensions with the same BD interferometer network, a deterministic multiphoton source, and joined multiphoton measurement. Multiple photons undergoing an interferometer network represent the walker in higher-dimensional structures and the polarization of the photons represents the coins manipulated by the wave plates. This opens a large unexplored field of research such as quantum simulation with multiple walkers.

In summary, we implement a stable and efficient way to realize 2D QW embedded in a broader framework and show that the position-dependent phase defects can influence the evolution of wave packets. The 2D QW with string phase defects has the wave functions of photons localized in certain lines. Here we observe localization on the lines instead of single points. Our experiment benefits from the high stability and full control of both coins and walkers at each step and in each given position. The versatility of our setup allows for extensions that would help us to study the topological structure of multidimensional QWs and develop applications such as quantum state transfer and energy transportation problems.

ACKNOWLEDGMENTS

This work has been supported by NSFC under Grants No. 11174052 and No. 11474049, and CAST Innovation fund. B.C.S. appreciates financial support from the 1000 Talent Plan of China, AITF, and NSERC.

APPENDIX: ISOMORPHISM BETWEEN TWO ONE-DIMENSIONAL QUANTUM WALKS AND ONE TWO-DIMENSIONAL QUANTUM WALK

In this Appendix we begin by describing the 1D QW, then describe a pair of 1D QWs with a shared coin [49] and follow with a discussion of the 2D QWs. Following these descriptions, we prove an isomorphism between a pair of 1D QWs sharing a quantum coin [49] and the 2D QW.

1. One-dimensional quantum walk

The 1D QW has a walker moving along an integer lattice whose sites are indexed by $x \in \mathbb{Z}$. Thus, the basis set for the walker state is $\{|x\rangle; x \in \mathbb{Z}\}$. The coin operator C^{1D} is an element of the Lie Group SU(2) and can be site dependent, which is important for introducing lattice defects. Therefore, we write the coin operator as

$$C^{1D} := \sum_{x\in\mathbb{Z}} |x\rangle\langle x| \otimes C^x \tag{A1}$$

to present site-dependent coin operation which is used widely in realizing generalized measurement via QWs [42], whereas non-site-dependent coin operation can be written as $\mathbb{1} \otimes C^x$ with $C^x \in$ SU(2) uniform for arbitrary x.

The coin-state basis is

$$\{|c\rangle \in P\mathbb{C}^2; c \in \mathbb{B}\} \tag{A2}$$

for $\mathbb{B} = \{0,1\}$ the bit space and $P\mathbb{C}^2$ the projective space of pairs of complex numbers. Thus, we can write

$$C^x = \begin{pmatrix} e^{-i\varphi^x}\cos\theta^x & e^{i\psi^x}\sin\theta^x \\ e^{-i\psi^x}\sin\theta^x & e^{i\varphi^x}\cos\theta^x \end{pmatrix} \tag{A3}$$

being the 2×2 complex matrix representation for SU(2), which is parametrized by three independent x-dependent angles θ^x, ψ^x, and φ^x.

The QW step operator U is obtained by combining the coin flip with the conditional translation of the walker. The conditional translation operator is

$$T^{1\mathrm{D}} = \sum_{x\in\mathbb{Z}} (|x\rangle\langle x+1| \otimes |0\rangle\langle 0| + |x+1\rangle\langle x| \otimes |1\rangle\langle 1|). \tag{A4}$$

The unitary QW step operator is thus

$$U^{1\mathrm{D}} = T^{1\mathrm{D}} C^{1\mathrm{D}}. \tag{A5}$$

The walker's evolution is obtained in discrete steps with evolution time given by

$$t \in \mathbb{N} = \{0,1,2,\ldots\}, \tag{A6}$$

and the evolution at time t is given by $(U^{1\mathrm{D}})^t$.

For fixed t, and for a walker whose state has support over a finite domain of $\{x \in \mathbb{Z}\}$, the step operator $U^{1\mathrm{D}}$ has a finite-dimensional representation. For the initial walker state commencing as a wholly localized state at the origin $x = 0$, the domain at time t can be restricted to

$$x \in \Delta_t := \{-t,\ldots,t\}. \tag{A7}$$

(Actually, the domain can be restricted to even and odd sublattices depending on the parity of t, but we ignore this simplification here.)

The 1D QW unitary step operator (A5) can be expressed as

$$\begin{aligned} U_t^{1\mathrm{D}} &= \sum_{x\in\Delta_t} (|x+1\rangle\langle x| \otimes |0\rangle\langle 0| + |x-1\rangle\langle x| \otimes |1\rangle\langle 1|) \\ &\quad \times \sum_{x'\in\Delta_t} |x'\rangle\langle x'| \otimes C^{x'} \\ &= \sum_{x\in\Delta_t}\sum_{c\in\mathbb{B}} |x+(-1)^c\rangle\langle x| \otimes (|c\rangle\langle c|C^x), \end{aligned} \tag{A8}$$

where we have employed the periodic boundary condition

$$|\pm(t+1)\rangle \equiv |\mp t\rangle. \tag{A9}$$

For

$$d_t^{1\mathrm{D}} := 2(2t+1), \tag{A10}$$

the operator U (A8) can be expressed as a $(d_t^{1\mathrm{D}} \times d_t^{1\mathrm{D}})$-dimensional special unitary matrix.

2. Two one-dimensional quantum walks

Now let us consider two 1D QWs, each holding a coin with site-dependent SU(2) operator. If the two QWs are completely independent of each other, the evolution is simply a power t of the tensor product of individual evolutions: $(U_t^{1\mathrm{D}} \otimes U_t^{1\mathrm{D}})^t$, which can be expressed as a special unitary matrix of dimension

$$\left(d_t^{1\mathrm{D}}\right)^2 \times \left(d_t^{1\mathrm{D}}\right)^2. \tag{A11}$$

The two-walker step-by-step unitary evolution operator is

$$\begin{aligned} U_t^{1\mathrm{D}1\mathrm{D}} &= T^{1\mathrm{D}1\mathrm{D}} C^{1\mathrm{D}1\mathrm{D}} \\ &= \sum_{x,y\in\Delta_t}\sum_{c,d,\in\mathbb{B}} |x+(-1)^c, y+(-1)^d\rangle\langle x,y| \\ &\quad \otimes (|c,d\rangle\langle c,d|C^{xy}), \end{aligned} \tag{A12}$$

where

$$\begin{aligned} T^{1\mathrm{D}1\mathrm{D}} &= \sum_{x,y\in\mathbb{Z}}\sum_{c,d,\in\mathbb{B}} |x+(-1)^c, y+(-1)^d\rangle\langle x,y| \\ &\quad \otimes |c,d\rangle\langle c,d|, \end{aligned} \tag{A13}$$

$$C^{1\mathrm{D}1\mathrm{D}} = \sum_{x,y\in\mathbb{Z}} |x,y\rangle\langle x,y| \otimes C^{xy}, \tag{A14}$$

and

$$C^{xy} \in \mathrm{SU}(4). \tag{A15}$$

This coin operator can be parametrized by 15 independent angles, and this operator (A12) reduces to $U_t^{1\mathrm{D}} \otimes U_t^{1\mathrm{D}}$ if

$$C^{xy} = C^x \otimes C^y \in \mathrm{SU}(2) \times \mathrm{SU}(2). \tag{A16}$$

Two independent walkers thus necessarily remain independent under this factorizable evolution.

If the coin operator (A15) is not factorizable, two walkers can become entangled by sharing coins, which is achieved by a fractional-swap operation

$$\begin{aligned} C^{xy} &= \Xi^{\tau^{xy}} \\ &= \frac{1}{2}\begin{pmatrix} 2 & 0 & 0 & 0 \\ 0 & 1+(-1)^{\tau^{xy}} & 1-(-1)^{\tau^{xy}} & 0 \\ 0 & 1-(-1)^{\tau^{xy}} & 1+(-1)^{\tau^{xy}} & 0 \\ 0 & 0 & 0 & 2 \end{pmatrix} \end{aligned} \tag{A17}$$

for Ξ the swap operator and $\tau^{xy} \in (0,1)$ [49]. If the walkers' coin-sharing procedure is independent of position, then $\tau^{xy} \equiv \tau$ (a constant). Thus, $U_t^{1\mathrm{D}1\mathrm{D}}$ (A12) can be expressed as a special unitary matrix of dimension $(d_t^{1\mathrm{D}})^2 \times (d_t^{1\mathrm{D}})^2$ the same as (A11).

3. Two-dimensional quantum walk

For a a single quantum walker moving along a 2D Cartesian lattice, a convenient basis choice is

$$\{|x,y,c\rangle; (x,y) \in \mathbb{Z}^2, c \in \mathbb{B}^2\}. \tag{A18}$$

Thus, the walk is over the 2D integer lattice and the coin-state parameter is given by a two-bit string.

Analogous to the 1D coin operator (A1), the 2D coin operator is

$$C^{2\mathrm{D}} := \sum_{(x,y)\in\mathbb{Z}^2} |x,y\rangle\langle x,y| \otimes C^{xy} \tag{A19}$$

to present a 2D site-dependent coin operator, whereas the non-site-dependent coin operation can be written as $\mathbb{1} \otimes C^{xy}$ with

C^{xy} uniform for any (x,y). Following the coin flip, translation takes place, which is given by the 2D translation operator

$$T^{\mathrm{2D}} = \sum_{(x,y)\in\mathbb{Z}^2} (|x,y\rangle\langle x+1,y| \otimes |0,0\rangle\langle 0,0| \\ + |x,y\rangle\langle x,y+1| \otimes |0,1\rangle\langle 0,1| \\ + |x,y+1\rangle\langle x,y| \otimes |1,0\rangle\langle 1,0| \\ + |x+1,y\rangle\langle x,y| \otimes |1,1\rangle\langle 1,1|). \tag{A20}$$

The unitary QW step operator is thus $U^{\mathrm{2D}} = T^{\mathrm{2D}}C^{\mathrm{2D}}$ analogous to the 1D translation operator (A4) and can be expressed as a $(d_t^{\mathrm{2D}} \times d_t^{\mathrm{2D}})$-dimensional special unitary matrix for

$$d_t^{\mathrm{2D}} := [2(2t+1)]^2 = \left(d_t^{\mathrm{1D}}\right)^2. \tag{A21}$$

The quantum walker accesses only the sub lattice $\Delta_t^{\otimes 2}$, which is a twofold tensor product of the 1D sublattice (A7).

4. Isomorphism between two one-dimensional quantum walks and one two-dimensional quantum walk

The isomorphism between two 1D quantum walkers and one 2D quantum walker is proven if the two transformations are identical in appropriate bases. We know from Eq. (A21) that the two matrices have the same size so the approach in this section is to find the appropriate basis transformation from 1D to 2D so the matrix representations are identical. Then we need to establish that the transformation (A23) and the two-coin operation including fractional swap (A17) leads to the same unitary step-operator matrix for the two cases of two 1D QWs and one 2D QW. We show this isomorphism by proving that

$$U_t^{\mathrm{1D1D}} = U_t^{\mathrm{2D}} \tag{A22}$$

after implementing the coördinate transformation (A23) and the fractional quantum-coin swap (A17).

We choose the mapping

$$x \mapsto x+y, \quad y \mapsto x-y, \tag{A23}$$

to carry coördinates x and y for the two 1D walkers to the joint coördinate of the 2D quantum walker. Under the transformation (A23), the 2D translation operator (A20) can be rewritten as

$$T^{\mathrm{2D}} = \sum_{x,y\in\mathbb{Z}} \sum_{c,d\in\mathbb{B}} |x+(-1)^c, y+(-1)^d\rangle\langle x,y| \\ \otimes |c,d\rangle\langle c,d|, \tag{A24}$$

which evidently matches T^{1D1D}—a crucial part of U_t^{1D1D} in Eq. (A12). The next step to proving the isomorphism is to decompose the SU(4) coin operator (A19) according to [55–57]

$$C^{xy} = (u_1 \otimes u_2)[(Z\otimes X)\Xi^{\gamma}(Z\otimes \mathbb{1}) \\ \times \Xi^{\beta}(\mathbb{1}\otimes X)\Xi^{\alpha}](v_1\otimes v_2) \tag{A25}$$

with Pauli matrices

$$X = \begin{pmatrix} 0 & 1 \\ 1 & 0 \end{pmatrix}, \quad Z = \begin{pmatrix} 1 & 0 \\ 0 & -1 \end{pmatrix}, \tag{A26}$$

general SU(2) elements $u_{1,2}$ and $v_{1,2}$, and Ξ^i ($i = \alpha,\beta,\gamma \in [0,1]$) the fractional-swap operation (A17). That is, an arbitrary SU(4) operation on a four-sided coin can be decomposed into three Ξ^i gates and single-qubit gates. An arbitrary SU(4) coin can be either separated or entangled. For the former case, C^{xy} can be decomposed into single-qubit gates only, i.e.,

$$C^{xy} = C^x \otimes C^y, \tag{A27}$$

if and only if

$$C^x = u_1 v_1, \quad C^y = u_2 v_2, \quad \alpha = \beta = \gamma = 0. \tag{A28}$$

For the latter case, C^{xy} can be decomposed by three Ξ^i gates, i.e.,

$$C^{xy} = \Xi^{\tau^{xy}} \tag{A29}$$

if and only if

$$\beta = \gamma = -1, \quad \alpha = \tau^{xy}, \quad u_{1,2} = v_{1,2} = \mathbb{1}. \tag{A30}$$

Thus we show the isomorphism between two 1D QWs with two walkers having separated coins and 2D QW with one walker controlling a four-sided coin in Eq. (A27), and the isomorphism between two 1D QWs with two walkers sharing coins and 2D QW with one walker controlling a four-sided coin in Eq. (A29) by proving $U_t^{\mathrm{1D1D}} = U_t^{\mathrm{2D}}$ for the two cases, respectively.

Therefore, a 2D QW with one walker controlled by a SU(4) coin flipping and a 1D QW with two walkers sharing coins [49] is proven to be isomorphic. Thus, one can use a 1D QW with two walkers to simulate 2D QW if the two walkers share their coins except for the local rotations.

Here we simulate a 2D walk with two 1D quantum walkers and treat the simple coin flipping operator $H^{\otimes 2}$ for Hadamard operator H, which is a special case of the coin operators for two 1D QWs (A16). In this case, the above coin operator for two 1D QWs is equivalent to that for a 2D QW C^{xy} in Eq. (A25) once

$$u_1 = u_2 = H, \quad \alpha = \beta = \gamma = 0, \quad v_1 = v_2 = \mathbb{1} \tag{A31}$$

are satisfied.

[1] Y. Aharonov, L. Davidovich, and N. Zagary, Phys. Rev. A **48**, 1687 (1993).

[2] A. Ambainis, Int. J. Quantum Inf. **01**, 507 (2003).

[3] A. M. Childs, R. Cleve, E. Deotto, E. Farhi, S. Gutmann, and D. A. Spielman, in *Proceedings of the 35th Annual ACM Symposium on Theory of Computing (STOC 2003)* (ACM, New York, 2003), pp. 59–68.

[4] N. Shenvi, J. Kempe, and K. Birgitta Whaley, Phys. Rev. A **67**, 052307 (2003).

[5] J. Kempe, Contemp. Phys. **44**, 307 (2003).

[6] A. M. Childs, Phys. Rev. Lett. **102**, 180501 (2009).

[7] A. M. Childs, D. Gosset, and Z. Webb, Science **339**, 791 (2013).

[8] N. B. Lovett, S. Cooper, M. Everitt, M. Trevers, and V. Kendon, Phys. Rev. A **81**, 042330 (2010).

[9] X. Zhan, H. Qin, Z.-H. Bian, J. Li, and P. Xue, Phys. Rev. A **90**, 012331 (2014).
[10] A. Schreiber, A. Gábris, P. P. Rohde, K. Laiho, M. Štefaňák, V. Potoček, C. Hamilton, I. Jex, and C. Silberhorn, Science **336**, 55 (2012).
[11] T. Kitagawa, M. S. Rudner, E. Berg, and E. Demler, Phys. Rev. A **82**, 033429 (2010).
[12] J. K. Asbóth, Phys. Rev. B **86**, 195414 (2012).
[13] T. Kitagawa, M. A. Broome, A. Fedrizzi, M. S. Rudner, E. Berg, I. Kassal, A. Aspuru-Guzik, E. Demler, and A. G. White, Nat. Commun. **3**, 882 (2012).
[14] A. C. Oliveira, R. Portugal, and R. Donangelo, Phys. Rev. A **74**, 012312 (2006).
[15] S. Hoyer, M. Sarovar, and K. B. Whaley, New J. Phys. **12**, 065041 (2010).
[16] A. Wójcik, T. Łuczak, P. Kurzyński, A. Grudka, T. Gdala, and M. Bednarska-Bzdega, Phys. Rev. A **85**, 012329 (2012).
[17] R. Zhang, P. Xue, and J. Twamley, Phys. Rev. A **89**, 042317 (2014).
[18] E. Segawa, J. Comput. Theor. Nanosci. **10**, 1583 (2013).
[19] Y. Yin, D. E. Katsanos, and S. N. Evangelou, Phys. Rev. A **77**, 022302 (2008).
[20] N. Konno, Quantum Inf. Process **9**, 405 (2010).
[21] Y. Shikano and H. Katsura, Phys. Rev. E **82**, 031122 (2010).
[22] A. Crespi, R. Osellame, R. Ramponi, V. Giovannetti, R. Fazio, L. Sansoni, F. De Nicola, F. Sciarrino, and P. Mataloni, Nat. Photonics **7**, 322 (2013).
[23] A. Schreiber, K. N. Cassemiro, V. Potoček, A. Gábris, I. Jex, and C. Silberhorn, Phys. Rev. Lett. **106**, 180403 (2011).
[24] P. Xue, H. Qin, and B. Tang, Sci. Rep. **4**, 4825 (2014).
[25] R. Zhang and P. Xue, Quantum Inf. Comput. **13**, 1825 (2014).
[26] A. Wójcik, T. Łuczak, P. Kurzyński, A. Grudka, and M. Bednarska, Phys. Rev. Lett. **93**, 180601 (2004).
[27] O. Buerschaper and K. Burnett, arXiv:quant-ph/0406039.
[28] M. C. Bañuls, C. Navarrete, A. Pérez, E. Roldán, and J. C. Soriano, Phys. Rev. A **73**, 062304 (2006).
[29] M. Genske, W. Alt, A. Steffen, A. H. Werner, R. F. Werner, D. Meschede, and A. Alberti, Phys. Rev. Lett. **110**, 190601 (2013).
[30] P. Xue, H. Qin, B. Tang, and B. C. Sanders, New J. Phys. **16**, 053009 (2014).
[31] J. Du, H. Li, X. Xu, M. Shi, J. Wu, X. Zhou, and R. Han, Phys. Rev. A **67**, 042316 (2003).
[32] F. Zähringer, G. Kirchmair, R. Gerritsma, E. Solano, R. Blatt, and C. F. Roos, Phys. Rev. Lett. **104**, 100503 (2010).
[33] H. Schmitz, R. Matjeschk, C. Schneider, J. Glueckert, M. Enderlein, T. Huber, and T. Schaetz, Phys. Rev. Lett. **103**, 090504 (2009).
[34] M. Karski, L. Förster, J.-M. Choi, A. Steffen, W. Alt, D. Meschede, and A. Widera, Science **325**, 174 (2009).
[35] R. Côté, A. Russell, E. E. Eyler, and P. L. Gould, New J. Phys. **8**, 156 (2006).
[36] P. Xue, B. C. Sanders, and D. Leibfried, Phys. Rev. Lett. **103**, 183602 (2009).
[37] P. Xue, B. C. Sanders, A. Blais, and K. Lalumiere, Phys. Rev. A **78**, 042334 (2008).
[38] D. Bouwmeester, I. Marzoli, G. P. Karman, W. Schleich, and J. P. Woerdman, Phys. Rev. A **61**, 013410 (1999).
[39] B. Do, M. L. Stohler, S. Balasubramanian, D. S. Elliott, C. Eash, E. Fischbach, M. A. Fischbach, A. Mills, and B. Zwickl, J. Opt. Soc. Am. B **22**, 499 (2005).
[40] H. B. Perets, Y. Lahini, F. Pozzi, M. Sorel, R. Morandotti, and Y. Silberberg, Phys. Rev. Lett. **100**, 170506 (2008).
[41] P. Xue, R. Zhang, H. Qin, X. Zhan, Z. H. Bian, J. Li, and B. C. Sanders, Phys. Rev. Lett. **114**, 140502 (2015).
[42] Z. H. Bian, J. Li, H. Qin, X. Zhan, R. Zhang, B. C. Sanders, and P. Xue, Phys. Rev. Lett. **114**, 203602 (2015).
[43] A. Schreiber, K. N. Cassemiro, V. Potoček, A. Gábris, P. J. Mosley, E. Andersson, I. Jex, and C. Silberhorn, Phys. Rev. Lett. **104**, 050502 (2010).
[44] L. Sansoni, F. Sciarrino, G. Vallone, P. Mataloni, A. Crespi, R. Ramponi, and R. Osellame, Phys. Rev. Lett. **108**, 010502 (2012).
[45] P. Xue and B. C. Sanders, Phys. Rev. A **87**, 022334 (2013).
[46] T. D. Mackay, S. D. Bartlett, L. T. Stephenson, and B. C. Sanders, J. Phys. A: Math. Gen. **35**, 2745 (2002).
[47] E. Roldán and J. C. Soriano, J. Mod. Opt. **52**, 2649 (2005).
[48] M. Annabestani, M. R. Abolhasani, and G. Abal, J. Phys. A: Math. Gen. **43**, 075301 (2010).
[49] P. Xue and B. C. Sanders, Phys. Rev. A **85**, 022307 (2012).
[50] A. Peruzzo, M. Lobino, J. C. F. Matthews, N. Matsuda, A. Politi, K. Poulios, X.-Q. Zhou, Y. Lahini, N. Ismail, K. Wörhoff, Y. Bromberg, Y. Silberberg, M. G. Thompson, and J. L. OBrien, Science **329**, 1500 (2010).
[51] K. Poulios, R. Keil, D. Fry, J. D. A. Meinecke, J. C. F. Matthews, A. Politi, M. Lobino, M. Gräfe, M. Heinrich, S. Nolte *et al.*, Phys. Rev. Lett. **112**, 143604 (2014).
[52] Y.-C. Jeong, C. Di Franco, H.-T. Lim, M. S. Kim, and Y.-H. Kim, Nat. Commun. **14**, 2471 (2013).
[53] M. A. Broome, A. Fedrizzi, B. P. Lanyon, I. Kassal, A. Aspuru-Guzik, and A. G. White, Phys. Rev. Lett. **104**, 153602 (2010).
[54] P. W. Anderson, Phys. Rev. **109**, 1492 (1958).
[55] B. Kraus and J. I. Cirac, Phys. Rev. A **63**, 062309 (2001).
[56] N. Khaneja, R. Brockett, and S. J. Glaser, Phys. Rev. A **63**, 032308 (2001).
[57] H. Fan, V. Roychowdhury, and T. Szkopek, Phys. Rev. A **72**, 052323 (2005).